19th International Conference
ENGINEERING MECHANICS 2013
Svratka, Czech Republic, May 13 – 16, 2013

EXTENSION OF SEMI-ANALYTICAL FRACTURE MODEL BASED ON THE COHESIVE CRACK APPROACH

T. Pail*, P. Frantík**

Abstract: *The paper presents the description of the developed JAVA implementation of the semi-analytical fracture model based on cracked hinge approach by Ulfkjær et al. (1995) and introduces generalization of the model formulation to enable using the tensile softening function with an arbitrary shape for the nonlinear part of the model assumed as cohesive crack. Performed simulations of an adopted wedge-splitting test show consistency of the new formulation with reference data. A comparison with FEM solution is also presented to demonstrate a dependency of a load-crack mouth opening curve obtained by FEM and the implemented hinge model on its band width for different choices of softening function.*

Keywords: ***hinge model, fracture, concrete, tensile softening, fracture energy.***

1. Introduction

Nowadays, one of main approaches commonly applied for a description of fracture behavior is the cohesive crack approach (Barenblat, 1962; Dugdale, 1963), further generalized by Hillerborg et al. (1976) for quasi-brittle materials such as concrete and other cement-based composites as the fictitious crack model (FCM). This model recognizes experimentally observed cohesive character of crack propagation which these materials exhibit—as the so-called material softening—due to microcracking and other related processes (e.g. crack bridging, aggregate interlocking). This phenomenon takes place within the extensive fracture process zone (FPZ) developed ahead of the tip of a real traction-free crack. The cohesive (fictitious) crack concept consider the fracture energy dissipated in the process zone via certain closing cohesive stress applied to the fracture surface of a fictitious extension of a real crack (called fictitious crack) approximating the FPZ. This stress is non-constant over the fictitious crack length and increase from zero at the tip of the real traction-free crack—with full separation of its faces—to a value of uniaxial tensile strength f_t of a material at the tip of the fictitious crack. Further a corresponding tensile softening function $\sigma(w)$ is introduced as the crack evolution property of the model describing the relationship between the magnitude of applied cohesive stress and crack opening displacement, w. Based on this arrangement the amount of fracture energy dissipated in FPZ is fully expressed as the work done by cohesive stress on the crack opening displacement. The review of the relevant references for this topic appears in (Bažant & Planas, 1998; Karihaloo, 1995).

The popularity and prevalence of models based on the cohesive crack approach is generally given by their simple implementation within the framework of the finite element method (FEM). Some well-known complex numerical tools for modelling both elastic (or elastic-plastic) behavior and the quasi-brittle fracture process have been developed on this basis, e.g. (Červenka et al., 2007). However, the practical using of such tools is limited by a trustworthy knowledge of the stress-crack opening relationship $\sigma(w)$ considered as the key material input. The straightforward approach to provide whole softening curve is through stable tensile tests. Unfortunately such direct experimental measurement is very difficult to perform, mainly because tests tend to shift to asymmetric modes of failure or because several cracks developed simultaneously. All of these influences can introduce significant error into measurements and make the obtained results unusable (van Mier & van Vliet, 2002).

* Ing. Tomáš Pail: Institute of Structural Mechanics, Brno University of Technology, Veveří 331/95; 602 00, Brno; CZ, e-mail: pail.t@fce.vutbr.cz

** Ing. Petr Frantík, Ph.D.: Institute of Structural Mechanics, Brno University of Technology, Veveří 331/95; 602 00, Brno; CZ; e-mail: kitnarf@centrum.cz

Application of indirect methods is another option to estimate softening curve from standardized fracture tests—the three-point bending test (TPBT) or the wedge splitting test (WST)—either using evaluation methods, e.g. the work of fracture method (RILEM, 1985), or increasingly used inverse analysis with the possible employment of advanced optimization techniques (Que, 2003). In the inverse analysis procedure, a set of parameters is provided as a seed for an iterative process, and numerical or analytical model is used to determine a corresponding load-displacement (*P*–*d*) or load-crack mouth opening displacement (*P*–CMOD) curve, which is compared with the referenced curve obtained from a laboratory test. Many strategies are possible for this task. Finite element models, available in academic or commercial packages, generate reliable solutions, although they are time consuming. Since these computations are performed many times for the fitting procedure, analytical or semi-analytical models seem to be more adequate, despite the expected loss of accuracy. In the present paper, the own implementation of the semi-analytical model based on the cracked hinge concept is introduced with some extensions as the example of effective numerical tool suitable for purposes of the inverse analysis.

2. The cracked hinge model

The idea of a cracked hinge was presented originally by Ulfkjær et al. (1995) as the analytical model for calculation of load–displacement curves of notched and un-notched beams, further developed by Stang & Olesen (1998, 2000). The basic assumption of the model is that presence of a crack influences overall stress and strain field of a structure only in a local manner and this discontinuity is expected to vanish outside the certain bandwidth, s. Thus, within this band a crack propagation is modelled as the fictitious crack, while outside, the rest of the structure is considered in terms of the classical elastic theory. This assumption implies a reduction of the computational cost since only part of a structure is calculated using ideally closed-form analytical solution for any piece-wise linear softening curve. To avoid difficulties with derivation of the analytical solution for more complex functions (poly-linear, exponential) and its implementation as code, the semi-analytical approach of Olesen & Østergaard (2006) was employed. Some additional improvements have been formulated by authors as well. Main reason for this modifications was to allow using an arbitrary softening curve without any significant increase in the computation costs in the global iterative scheme.

2.1. Theoretical basis

The cracked hinge model can be viewed as a set of independent spring elements which are formed by incremental horizontal strips of the predetermined area of the structure surrounding a propagating crack, see Fig. 1. The flexural deformation are concentrated within this isolate domain modelled generally as a non-linear material hinge.

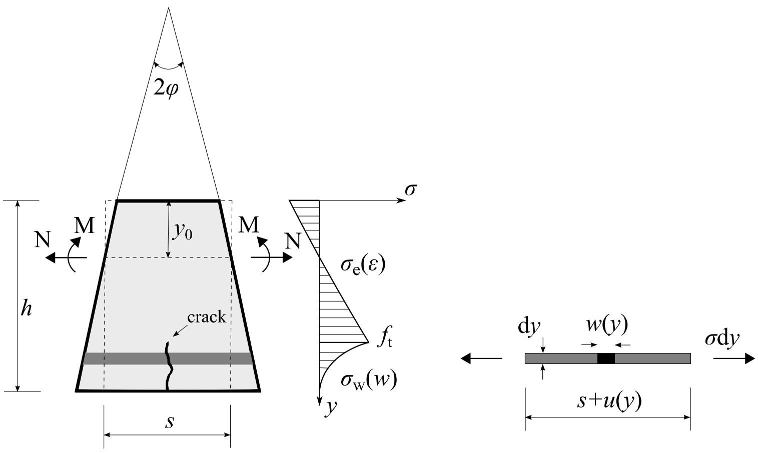

Fig. 1: Loading and deformation of the cracked hinge element with stress distribution (left) and incremental layer inside the hinge considered as the non-linear spring (right).

Due to rotation and translation of the rigid boundary of the hinge, the length of the attached springs is changed. The response of the springs on an enforced deformation is then considered linear elastic for pre-cracked state of a spring, whereas the cracked state is approximated by selected softening curve. Thus the stress distribution (see Fig. 1 left) can be determined by the equation:

$$\sigma(y) = \begin{cases} \sigma_{\mathrm{e}}(\varepsilon) = E\varepsilon & \text{pre-cracked state,} \\ \sigma_{\mathrm{w}}(w) & \text{cracked state,} \end{cases} \tag{1}$$

where E denotes the elastic modulus and ε elastic strain.

For evaluation of the stress distribution, a knowledge of the deformation state of the hinge is necessary to determine. This state is uniquely defined by a value of the angular deformation 2φ and by position of the neutral axis, y_0. Thus, based on assumptions above, the strain distribution can be simply obtained from the expression:

$$\varepsilon(y) = 2\varphi(y - y_0)/s. \tag{2}$$

A total elongation of any spring $u(y)$ located at the distance y subsequently depends on two possible contributions. The first one is via an elastic strain $\varepsilon(y)$ and second one is due to a crack opening, $w(y)$. Thus, $u(y)$ is given by nonlinear equation

$$u(y) = s\varepsilon(y) = s\frac{\sigma_{\mathrm{w}}(w(y))}{E} + w(y), \tag{3}$$

which is necessary to solve numerically in the case of requirement of using arbitrary softening curve, e.g. as a root finding algorithm for the function

$$f(w(y)) = s\varepsilon(y) - s\frac{\sigma_{\mathrm{w}}(w(y))}{E} - w(y). \tag{4}$$

2.2. Application to WS specimens

Generally the hinge model can be incorporated to any structure with crack subjected to a bending moment (possibly combined with normal force). Such an example is also the wedge splitting test. The modelling of the wedge splitting specimen (see Fig. 2) using the hinge model was pioneered by Østergaard (2003). Since then, more authors have used same approach, mostly as a subroutine of the above-mentioned inverse analysis (Abdalla & Karihaaloo, 2004; de Oliveira e Sousa & Gettu, 2006; Skoček & Stang, 2008). Let us add that only bilinear or polylinear type of softening curve have been used in these cases.

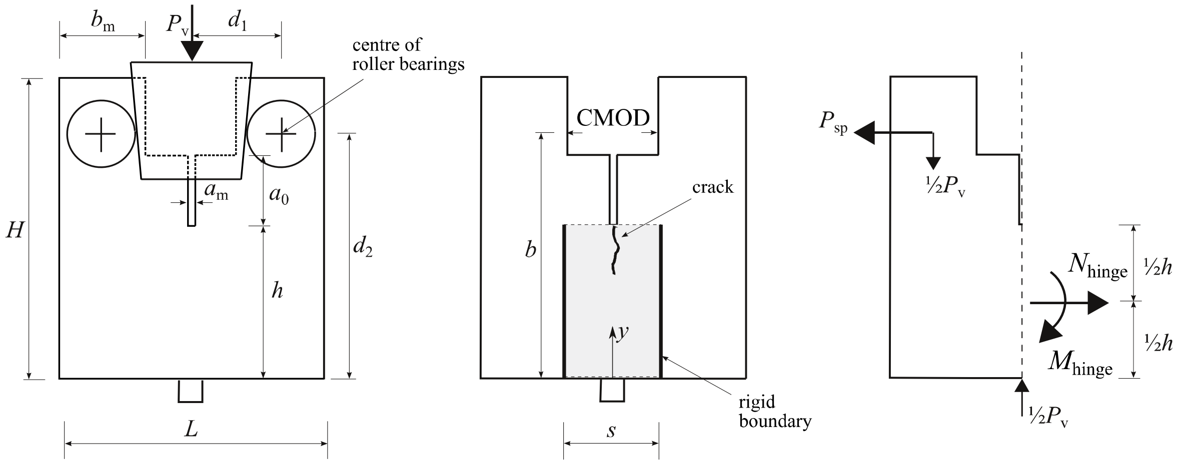

Fig. 2: Geometry and the loading of wedge splitting specimen with incorporated hinge element.

The example of wedge splitting test have been chosen also in this paper for the validation of the presented implementation of the hinge model, in this time using an arbitrary softening curve. Fig. 2 shows the incorporation of the hinge element in the WST specimen. The output of the wedge splitting test typically consists of the record of the loading force P depending on the crack mouth opening displacement (CMOD) measured at the point of the load application. For the determination of P–CMOD diagram we come from the fact that for a given values of angular deformation and neutral axis position of the hinge we can simply evaluate its transmitted bending moment M_{hinge} and normal force N_{hinge} by the following expressions

$$N_{\text{hinge}} = t\int_0^h \sigma(y)dy = \sum_{i=1}^{n} F_i,$$
$$M_{\text{hinge}} = t\int_0^h \sigma(y)(y-y_0)dy = \sum_{i=1}^{n} F_i(y_i - y_0), \tag{5}$$

where the stress distribution $\sigma(y)$ is defined from Eq. 1 and t denotes thickness of the specimen. According to the considered discretization (see Fig. 1), the F_{i} (Eq. 5) represents a magnitude of the force transmitted by i-th spring which can be quantified as

$$F_i = \sigma(y_i)t\text{d}y. \tag{6}$$

The key part of the hinge model algorithm is to determine the neutral axis position for a chosen angular deformation of the hinge element using the equilibrium conditions

$$M_{\text{hinge}} = M_{\text{ext}} \ \text{ a } \ N_{\text{hinge}} = P_{\text{sp}}. \tag{7}$$

Here the M_{ext} stands for the bending moment invoked by an applied loading, namely by its sectional components—vertical force P_{v} and splitting force P_{sp}—showing in Fig. 2 (right). The magnitude of M_{ext} we can expressed, neglecting self-weight of the specimen, by equation

$$M_{\text{ext}} = P_{\text{sp}}(d_2 - y_0) + \frac{1}{2}P_{\text{v}}d_1, \tag{8}$$

where the vertical force, P_{v}, we determine for a values of wedge angle α_{w} and coefficient of friction in the roller bearings μ_{c} as

$$P_{\text{v}} = P_{\text{sp}}\frac{2\tan\alpha_{\text{w}} + \mu_{\text{c}}}{1-\mu_{\text{c}}\tan\alpha_{\text{w}}}. \tag{9}$$

The summary of the algorithm of the calculation of a position of the neutral axis follows:

1)	Definition of geometry and material properties of a modelling specimen
2)	Setting the initial value of the angular deformation of the model (2φ)
3)	Subroutine for the calculation of the position of the neutral axis (y_0):
	Do
	Setting the value of the neutral axis as a result from a previous iteration step (the initial value is $h/2$)
	Loop over the springs (n = count of spring):
	For ($i = 0$; $i < n$; i++)
	Evolution of strain for the i-th spring (Eq. 2)
	Numerical calculation of the crack opening for the i-th spring (Eq. 4)
	Determination of stress and force transmitted by the i-th spring (Eq. 1)
	Evaluation of internal forces transmitted by the hinge (M_{hinge}, N_{hinge}), see Eq. 5
	Evaluation of external loading forces applied to the hinge model (P_{sp}, P_{v}, M_{ext}), see Eq. 7-9
	While ($\lvert M_{\text{hinge}} - M_{\text{ext}}\rvert$ < ERROR).

The CMOD, here defined as the opening of the specimen at the line of loading, depends on three different contributions. The first contribution, δ_{e}, is caused via elastic deformation of the specimen. The second one is due to the crack opening emanating from the starter crack/notch, δ_{w}. Finally, the third contribution is caused by the fact that there is a certain distance from the crack mouth located at h, to the line where CMOD is measured located at point b. This geometrical amplification, δ_{g}, is expressed through the estimation of the rotation of the crack faces. Thus, CMOD, is given by

$$\text{CMOD} = \delta_{\text{e}} + \delta_{\text{w}} + \delta_{\text{g}}. \tag{10}$$

For evaluation of the first term in Eq. 10 the formula found in Tada et al. (1985) can be used

$$\delta_{\text{e}} = \frac{P_{\text{sp}}}{Et}v_2(x), \tag{11}$$

where $v_2(x)$ represents geometric function computed for $x = 1 - h/b$ as follows

$$v_2(x) = \frac{x}{(1-x)^2}(38.2 - 55.4x + 33.0x^2). \tag{12}$$

The second term in Eq. 10, δ_w, can be directly evaluated form the Eq. 4 at point $y = h$. The last term, δ_g, is derived differently than in Østergaard (2003) as simplified formula

$$\delta_g = (b-h)\frac{\delta_w}{h} \tag{13}$$

based on the assumption that "average" value of the angle between crack faces, θ_w, is expressed as $\theta_w = \delta_w / h$.

3. Results and discussion

The above-mentioned procedures were implemented in programming language JAVA and afterwards validated by results published earlier in literature (Østergaard (2003)). The referenced WST specimen for performed simulations was with these dimensions: $L = H = 100$ mm; $h = 50$ mm; $a_0 = 28$ mm; $d_1 = 35$ mm; $d_2 = 85.2$ mm; $a_m = 4.5$ mm; $b_m = 35$ mm; thickness $t = 100$ mm (the dimensions are indicated in Fig. 2 left). The angle of the wedge was chosen as $\alpha_w = 15°$ and friction in the roller bearings was ignored, so that $\mu_c = 0$. The elastic un-cracked part of the modelled specimen was prescribed by Young's modulus $E = 30$ GPa and Poisson's ratio $\nu = 0.2$. The fictitious crack part was defined by referenced tensile softening as the bilinear diagram with parameters: tensile strength $f_t = 2$ MPa; critical crack opening $w_c = 0.5$ mm; coordinates of the kink point $\sigma(w_1) = 0.2$ MPa and $w_1 = 0.045$ mm; fracture energy $G_F = 95.5$ Nm. The hinge model was loaded by incremental value of the angular deformation $\Delta\varphi = 1.0\times10^{-5}$ rad.

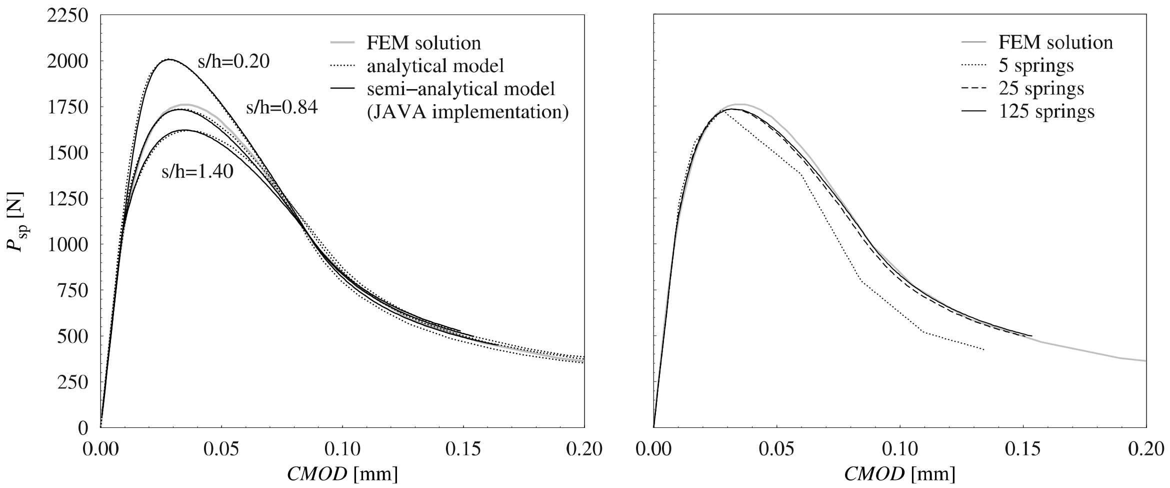

Fig. 3: Comparison of the P–CMOD response of the implemented semi-analytical model with data of FEM and analytical solution originally published by Østergaard (left); convergence study of the implemented model shown on P–CMOD diagram (right).

For the referenced configuration, the computed *P*-CMOD diagrams, see Fig. 3 (left), shows the consistency of a response with the analytical model by Østergaard (2003). Observed small discrepancies are probably caused by the modification of the CMOD calculation procedure which is represented by Eq. 13. The study shown in Fig. 3 (right) documents very fast convergence of the hinge model depending on the increasing count of the springs. Apparently the rate of convergence will depend mainly on a prescribed softening function curve.

In order to investigate capability of the implemented model to use any softening curve with arbitrary shape, the following numerical study is presented. From previous results it is obvious that explicit value of the hinge bandwidth, *s*, is necessary to calibrate if we required optimal agreement with FEM solution. Therefore, the comparison of simulation results from two models, implemented cracked hinge model and specialized own-developed academic-purpose FE code implemented the FCM, is further discussed. In this study, the following type of tensile softening function were used, see

Fig. 4 (left): bilinear (referenced); linear and Hordijk's power exponential function according to formula

$$\sigma(w) = f_t \left\{ \left[1 + \left(a_1 \frac{w}{w_c} \right)^3 \right] \exp\left(-a_2 \frac{w}{w_c} \right) - \frac{w}{w_c} \left(1 + a_1^3 \right) \exp\left(-a_2 \right) \right\} \tag{14}$$

with coefficients $a_1 = 3$, $a_2 = 6.93$ and critical crack opening $w_c = 5.136 G_F/f_t$.

The FE mesh illustrated in Fig. 4 (right) consist of linear elastic isoparametric quadrilateral elements in plane stress with parameters mentioned earlier. The FE simulation was controlled by stable CMOD control (ΔCMOD = 2.5×10^{-4} mm) with simultaneously applied vertical loading force $½P_v$ recalculated iteratively for each loading step. The additional loading by cohesive force was applied under the conditions of the FCM.

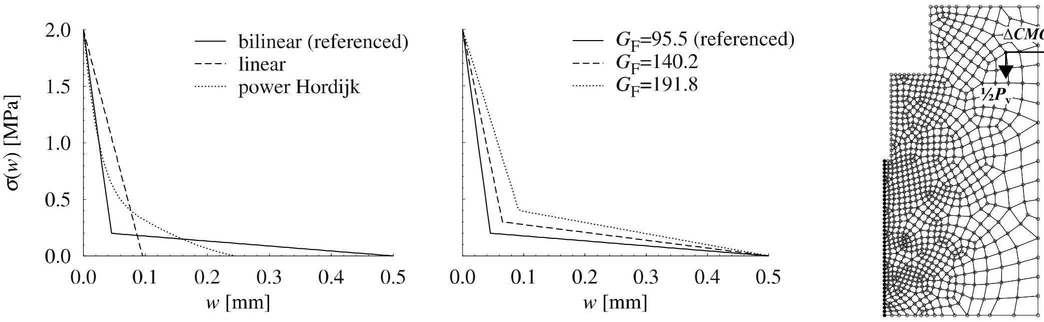

Fig. 4: The defined tensile softening functions: with constant (left) and increasing (middle) value of the fracture energy; FE mesh of the WST specimen (right).

The first set of results (Fig. 5, left) were obtained for the defined tensile softening functions according to Fig. 4 (left) with considered constant value of tensile strength f_t = 2.0 MPa and fracture energy G_F = 95.5 N/m. The explicit band width of the WS specimen as the characteristic size of the hinge element was fixed in ratio s/h = 0.64. Let us add that this value is optimal value (based on FEM comparison) in the case of the referenced bilinear softening curve. From these results it is evident that pure change of the shape of a softening function caused relatively small deviation from corresponding FEM solution. Similar behavior is viewed in Fig. 5 (right) where the second set of results were obtained this time for increasing value of the fracture energy in case of bilinear functions illustrated in Fig. 4 (middle). The major discrepancy between the *P*–CMOD diagrams is concentrated around the peak load and confirms the fact that elastic energy stored in the crack band increases with increasing band width *s* and thus, results in a more unstable crack growth, yielding a lower peak value. The overall curve then remains unchanged except the amount of the fracture energy G_F needed to be preserved constant.

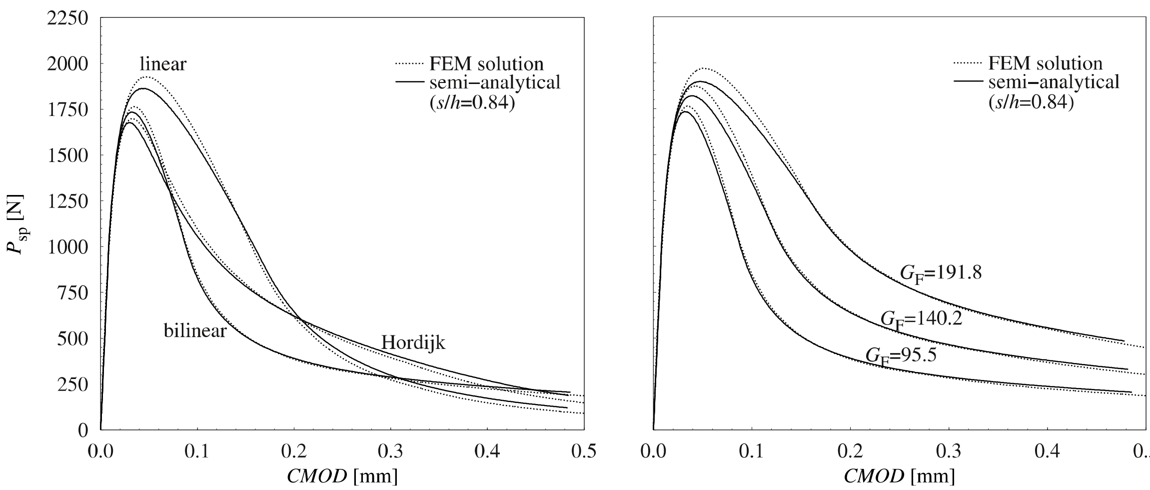

Fig. 5: Simulated P–CMOD diagrams of the models using the defined tensile softening functions with the constant (left) and increasing (right) fracture energy.

4. Conclusion

The paper presents the description of the author's implementation (in JAVA programming language) of semi-analytical fracture model based on the cracked hinge approach introduced by Ulfkjær et al. (1995) and further developed by Stang & Olesen (1998, 2000). Generalized formulation of this model was adopted which enables to use for the cracked part of a structure described as the fictitious (cohesive) crack the tensile softening function with an arbitrary shape. The implemented procedures were validated by data published by Ostergaard (2003) where a wedge splitting test had been simulated. The obtaining results correspond with this origin data and confirm the applicability of the implemented model. The general dependency of band width of the hinge element incorporated to the WS specimen was also presented in the numerical study involving FEM modelling. There, the influence of the change of a tensile softening function shape and increasing value of fracture energy was investigate and indicates that this dependency is not strong but implies the necessity to calibrate the hinge model when we required optimal agreement with a FEM solution.

Acknowledgements

The financial support received from the Czech Science Foundation under Project No. P105/11/1551 and specific research program of Brno University of Technology under Project No. FAST/J/13/1938 is gratefully acknowledged.

References

Abdalla, H. M. & Karihaloo, B. L. (2004) A method for constructing the bilinear tension softening diagram of concrete corresponding to its true fracture energy. *Magazine of Concrete Research*, Vol. 10, pp. 597–604.

Barenblatt, G. I. (1962) Mathematical theory of equilibrium cracks in brittle fracture. *Advances in Applied Mechanics*, Vol. 7, pp. 55–129.

Bažant, Z. P. & Planas, J. (1998) Fracture and Size Effect in Concrete and other Quasi-brittle Materials. CRC Press, Boca Raton, Florida.

Červenka, V., Jendele, L. & Červenka, J. (2007) ATENA Program documentation – Part 1: theory. Červenka Consulting, Prague.

De Oliveira e Sousa J. L. A. & Gettu, R. (2006) Determining the Tensile Stress-Crack Opening Curve of Concrete by Inverse Analysis. *ASCE Journal of Engineering Mechanics*, Vol. 132, pp. 141-148

Dugdale, D. S. (1960) Yielding of steel sheets containing slits. *J Mech Phys Solids*, Vol.8, pp. 100-108.

Hillerborg, A., Modeer, M. & Petersson, P. E. (1976). Analysis of crack formation and crack growth in concrete by means of fracture mechanics and finite elements. *Cem. Concr. Res*., Vol. 6, pp. 773–782.

Karihaloo, B. L. (1995) Fracture mechanics of concrete. Longman Scientific & Technical, New York.

Olesen, J. F. & Østergaard L. (2006) Method for determination of tensile properties of ECC – i: formulation and parameter variations, in*: International RILEM workshop on high performance fiber reinforced cementitious composites in structural applications.* RILEM Publications SARL, pp.47-55.

Østergaard L. (2003). Early-age fracture mechanics and cracking of concrete. *PhD Thesis*, Department of Civil Engineering, Technical University of Denmark, Lyngby, Denmark.

Que, N. S. (2003). Identification of cohesive crack fracture parameters using mathematical programming. *PhD Thesis,* School of Civil and Environmental Engineering, The University of New Wales, Sydney, Australia.

RILEM Committee FMT 50 (1985) Determination of the fracture energy of mortar and concrete by means of three-point bend test on notched beams. *Mater. Struct*., Vol. 18, pp. 285–290.

Skoček, J. & Stang, H. (2008) Inverse analysis of the wedge-splitting test. *Eng. Fract. Mech.*, Vol. 78, pp. 3173-3188.

Stang, H. & Olesen, J. F. (1998) On the interpretation of bending tests on FRC materials. *Journal of Sound and Vibration*, 218, 5, pp.123-132.

Stang, H. & Olesen, J. F. (2000) A fracture mechanics based design approach to FRC, in*: Proc. Fifth RILEM symposium on Fibre-Reinforced Concretes* (P.Rossi & G.Chanvillard eds), RILEM, Cachan, France, pp.315-324.

Ulfkjær, J. P., Krenk, S. & Brincker, R. (1995) Analytical model for fictitious crack propagation in concrete beams. *ASCE Journal of Engineering Mechanics*, Vol. 121, pp.7-15.

Van Mier, J. G. M. & Van Vliet, M. R. A. (2003). Influence of microstructure of concrete on size/scale effects in tensile fracture. *Engineering Fracture Mechanics*, Vol. 70, pp. 2281–2306.